Supplementary Material of

Evaluation of Anthropogenic Emissions and Ozone Pollution in the North China Plain: Insights from the Air Chemistry Research in Asia (ARIAs) Campaign

Hao He[1], Xinrong Ren[1,2,3], Sarah E. Benish[1], Zhanqing Li[1,4,5], Fei Wang[5,6], Yuying Wang[5], Timothy P. Canty[1], Xiaobo Dong[7], Feng Lv[7], Yongtao Hu[8], Tong Zhu[9], and Russell R. Dickerson,[1,4]

[1]Department of Atmospheric and Oceanic Science, University of Maryland, College Park, MD 20742, USA

[2]Air Resources Laboratory, National Oceanic and Atmospheric Administration, College Park, MD 20742, USA

[3]Cooperative Institute for Climate and Satellites, University of Maryland, College Park, Maryland, USA

[4]Earth System Science Interdisciplinary Center, University of Maryland, College Park, MD 20740, USA

[5]College of Global Change and Earth System Science, Beijing Normal University, Beijing, 100875, China

[6]Key Laboratory for Cloud Physics, Chinese Academy of Meteorological Sciences, Beijing, 100081, China

[7]Weather Modification Office of Hebei Province, Shijiazhuang, 050021, China

[8]School of Civil & Environmental Engineering, Georgia Institute of Technology, Atlanta, GA 30332, USA

[9]College of Environmental Sciences and Engineering, Peking University, Beijing 100871, China

Table S1 shows the aircraft instrumentation on the Y12 aircraft during ARIAs. For synchronization of aircraft measurements, we first synchronized Picarro measurements of CO_2, CO and CH_4, which have a 6-second lag time that takes for a plume to transport from the aircraft sample inlet to the Picarro cavity to be detected the analyzer. The lag time was determined by introducing a pulse of CO_2/CO/CH_4 calibration standard into the sample inlet and then measure the time it takes for the Picarro detects the pulsed signals. All other measurements were then synchronized based on concurrent peak appearance of these measurements and the Picarro measurements.

Table S1. UMD Aircraft Instrumentation

Variable	**Method**	**Sample Frequency**	**Precision/Accuracy***
Position	GPS	1 s	Horizontal: ~1 / ±2.5 m Vertical: ~1 / ±3.75 m
Meteorology (T, RH, P, 2-D Wind)	Cloud water inertial probe (CWIP): Hotwire, advanced heading reference system, 5-hole gust probe	1 s	T: 0.2 / ±0.5 °C P: 2.6 hPa / ±0.25% of FS RH: 1 / ±2% WS: 0.5 / ±1.0 m/s WD: 5 / ±10 °
Greenhouse gas CO_2/CH_4/CO/H_2O	Cavity Ring Down Spectroscopy Picarro Model G2401-m	2 s	CO_2: 0.02 / ±0.1 ppm CH_4: 0.2 / ±1 ppb CO: 4.2 / ±10 ppb
Ozone (O_3)	UV Absorption	10 s	1 ppb / ±1%
Sulfur Dioxide (SO_2)	Pulsed Fluorescence	10 s	0.1 ppb / ±3%
Nitrogen Dioxide (NO_2)	Cavity enhanced absorption spectroscopy, Los Gatos	1 s	0.05 ppb / ±5%
Reactive Nitrogen (NO-NOy)	Chemiluminescence	10 s	0.05 ppb / ±3%
Aerosol Scattering, b_{scat} (450, 550, 700 nm)	Nephelometer	1 s	$\pm 5x10^{-7}$ m^{-1} / ±5%
Aerosol Absorption, b_{abs} (565 nm)	Particle Soot Absorption Photometer (PSAP)	1 min	$\pm 5x10^{-7}$ m^{-1} / ±5%
Black Carbon (370, 470, 520, 590, 660, 880, 950 nm)	Aethalometer	2 min	0.05 $\mu g/m^3$ / ±5%
VOCs	Grab Canisters/GC-FID	5-6 / flight	Species dependent
Formaldehyde	Wet chemistry and fluorescence detection	90 seconds	0.1 ppb / ±5%

*The precisions are from the instrument specifications provided by the manufacturers while the accuracies are estimated from the uncertainties in calibration standards and mass flow controllers that are used to control flow rates of zero air and calibration gas.

Figure S1. ARIAs flights over the NCP and the WRF-CMAQ domains. Eleven Research Flights were conducted in May to Mid-June 2016.

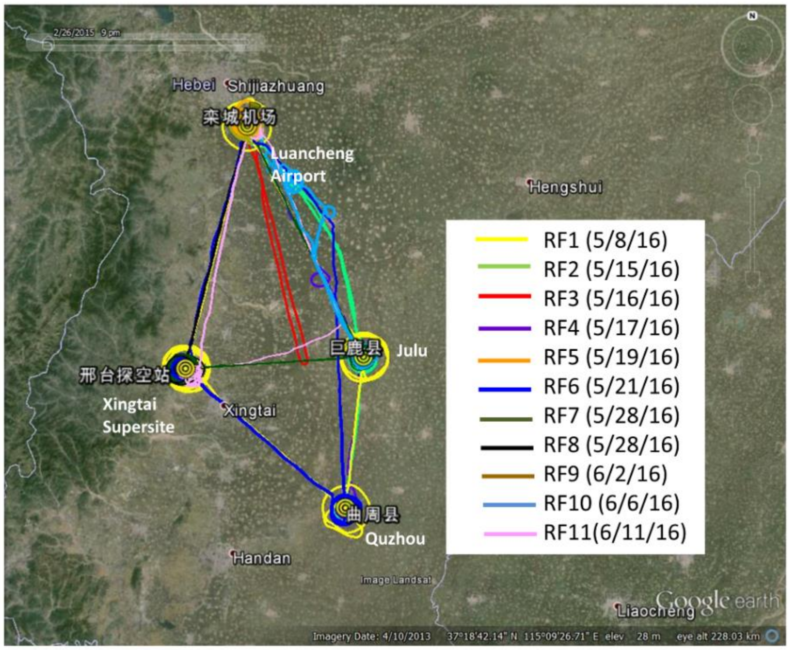

Figure S2. A plume observed over Xingtai during the flight on June 11, 2016. The height of mixing layer is around 1500 m AGL. Secondary peaks NO_2 at 500 m AGL and CO at 1500 m AGL were observed.

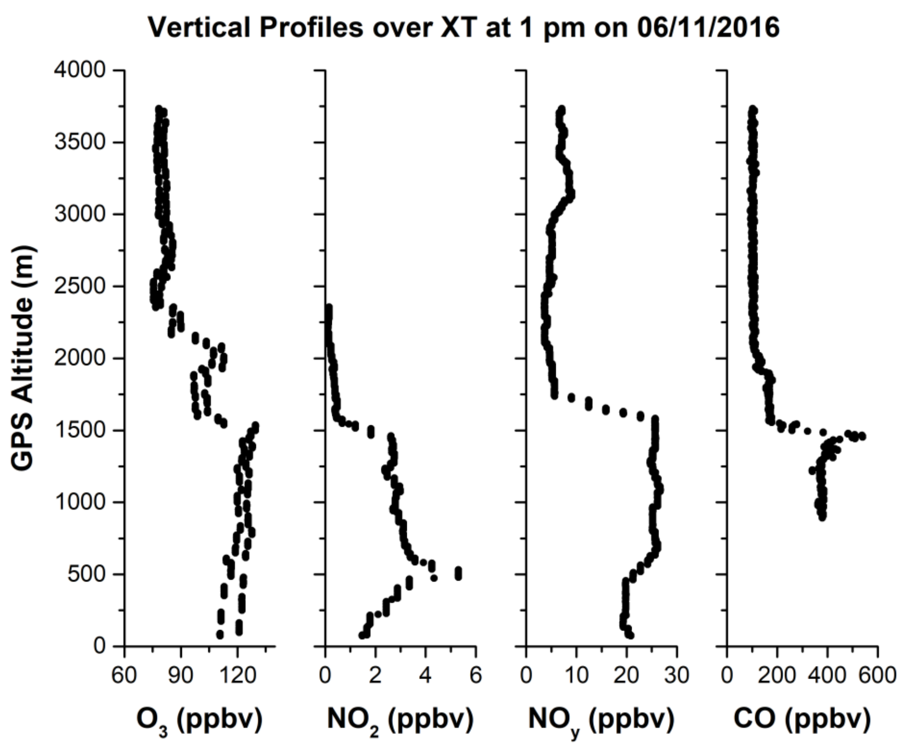

Figure S3. Comparison of surface hourly observations of air pollutants and CMAQ simulations at the Xingtai supersite from May to mid-June 2016. a) O_3, b) CO, c) NO_2^*, d) NO_x and e) HCHO. *Surface NO_2 is inferred as NO_x-NO from surface observations.

a)

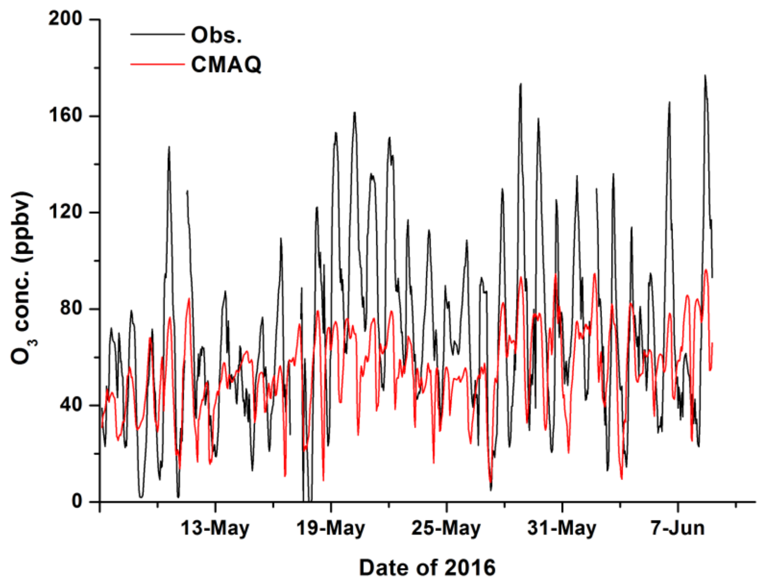

b)

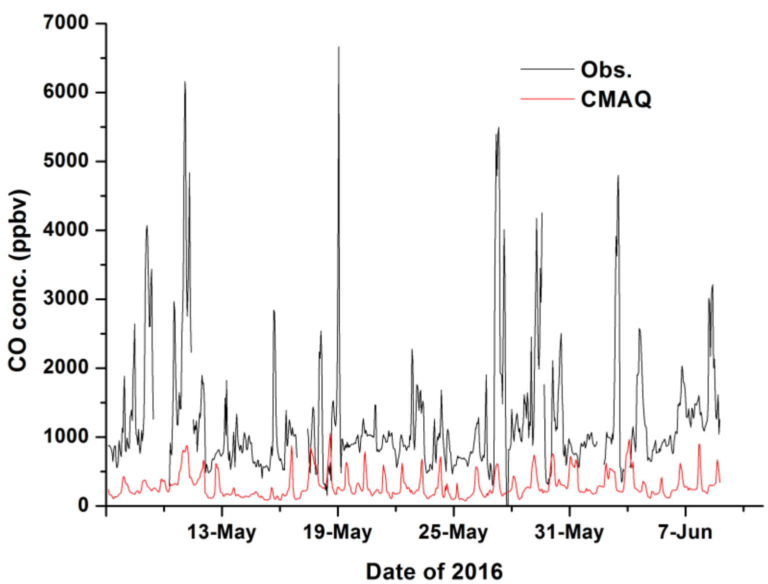

c)

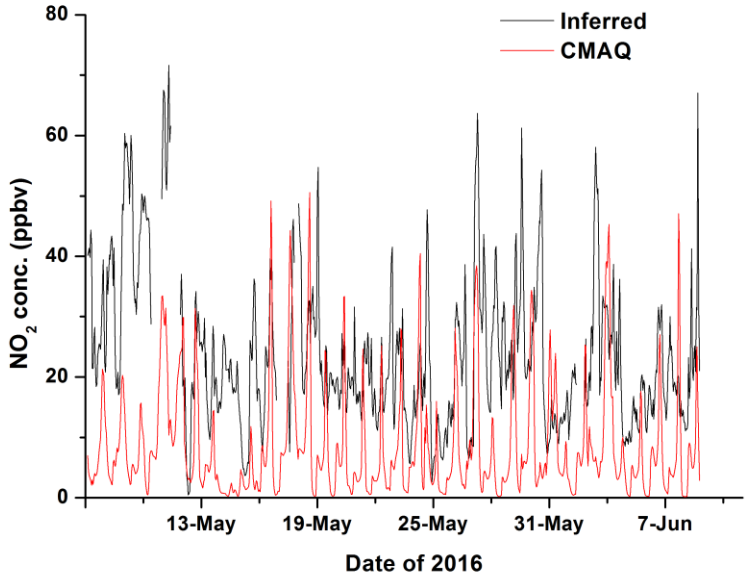
Inferred
CMAQ
NO_2 conc. (ppbv)
0
20
40
60
80
13-May
19-May
25-May
31-May
7-Jun
Date of 2016

d)

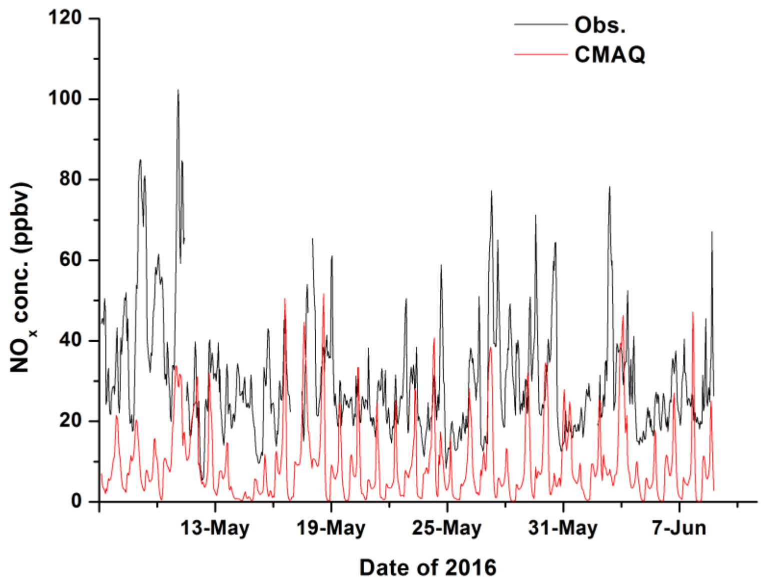
Obs.
CMAQ
NO_x conc. (ppbv)
0
20
40
60
80
100
120
13-May
19-May
25-May
31-May
7-Jun
Date of 2016

e)

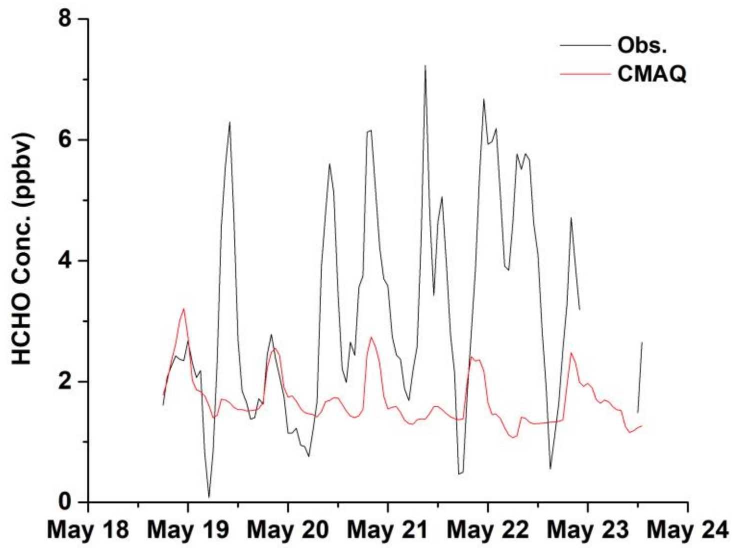

Figure S4. Terrain map of the Xingtai supersite (Picture obtained from Google Earth). The supersite is located on a small hill surrounded by mountains to the west. The Xingtai city (with ~ 1 million population) is located ~15 km southeast of the supersite.

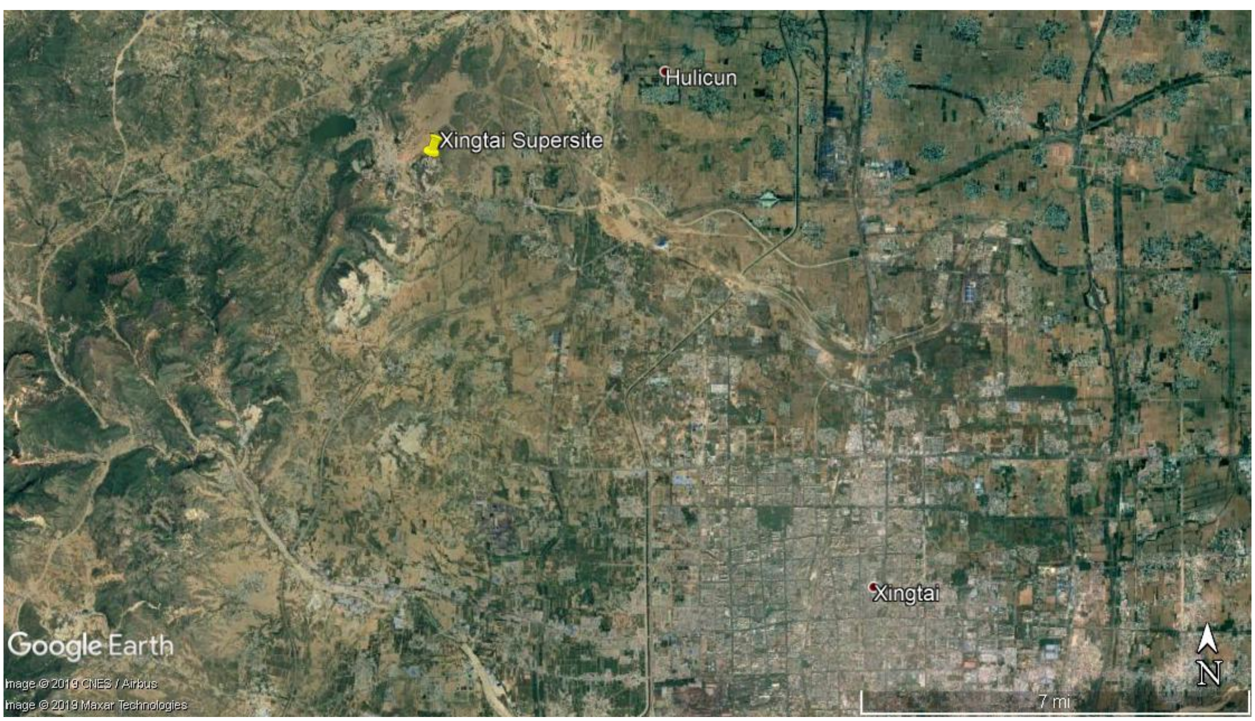

Figure S5. A case study comparing aircraft observations and the baseline CMAQ modeling results on June 11, 2016. Background: CMAQ simulations. Overlay: 1-min Y12 measurements. a) O_3, b) NO_2, c) NO, d) NO_y, e) CO.

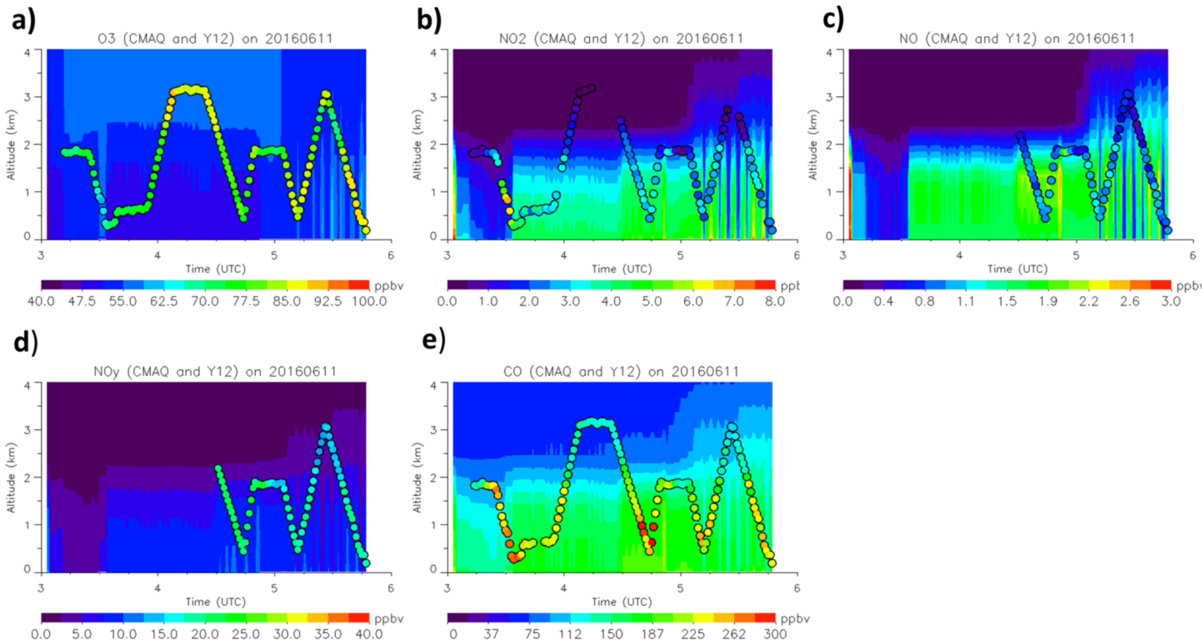

Figure S6. Ratios of column contents of the baseline CMAQ simulations and satellite observations. a) CMAQ/OMI NO_2; b) CMAQ/OMI HCHO; c) CMAQ/MOPITT CO.

a)

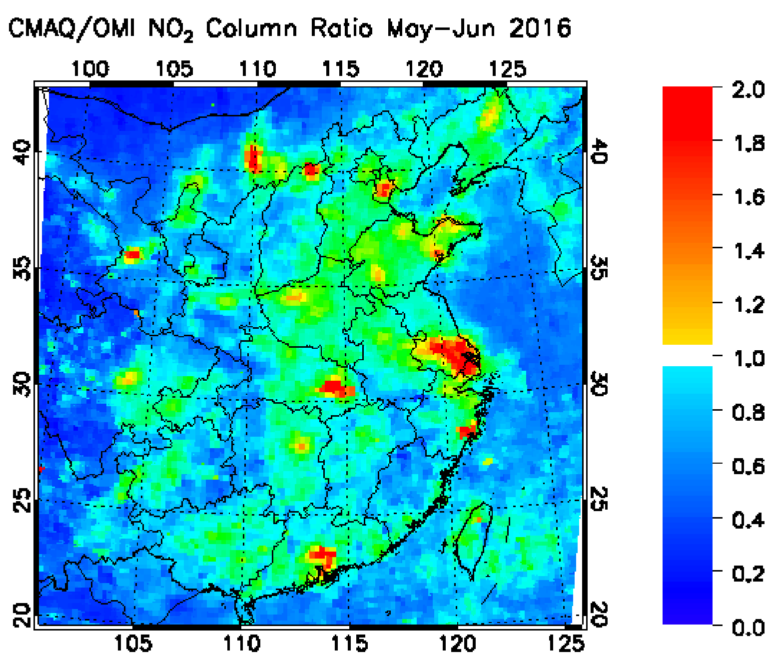

b)

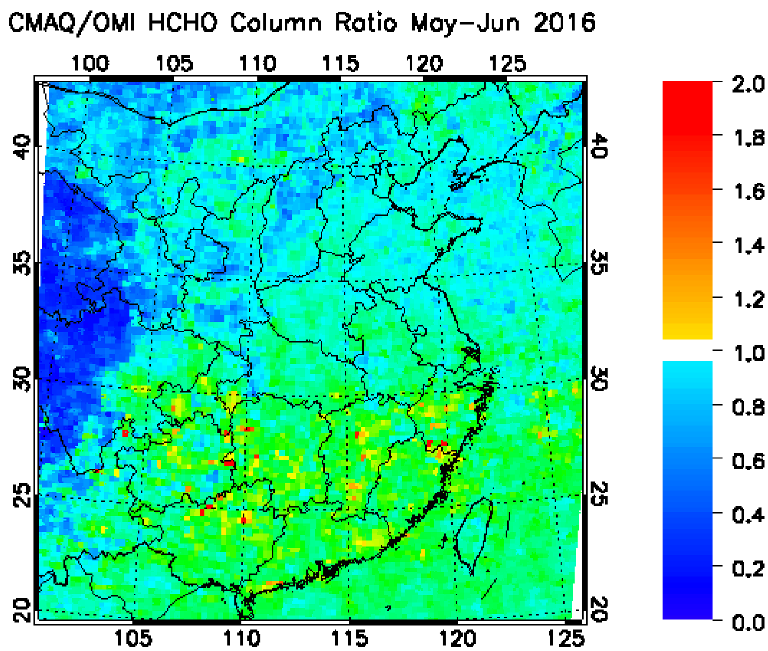
CMAQ/OMI HCHO Column Ratio May–Jun 2016
100
105
110
115
120
125
40
35
30
25
20
105
110
115
120
125
2.0
1.8
1.6
1.4
1.2
1.0
0.8
0.6
0.4
0.2
0.0

c)

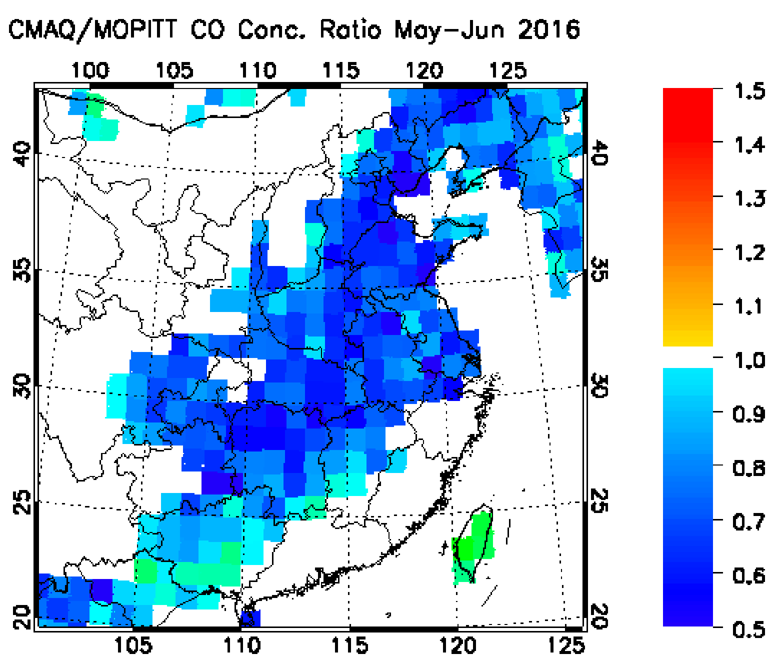
CMAQ/MOPITT CO Conc. Ratio May–Jun 2016
100
105
110
115
120
125
40
35
30
25
20
105
110
115
120
125
1.5
1.4
1.3
1.2
1.1
1.0
0.9
0.8
0.7
0.6
0.5

Figure S7. Similar as Figure 7, but shows differences between satellite observations and CMAQ simulations in May and June 2016. a) difference of NO_2 column between OMI and CMAQ; b) difference of HCHO column between OMI and CMAQ; c) difference of near surface CO between MOPITT and CMAQ.

a)

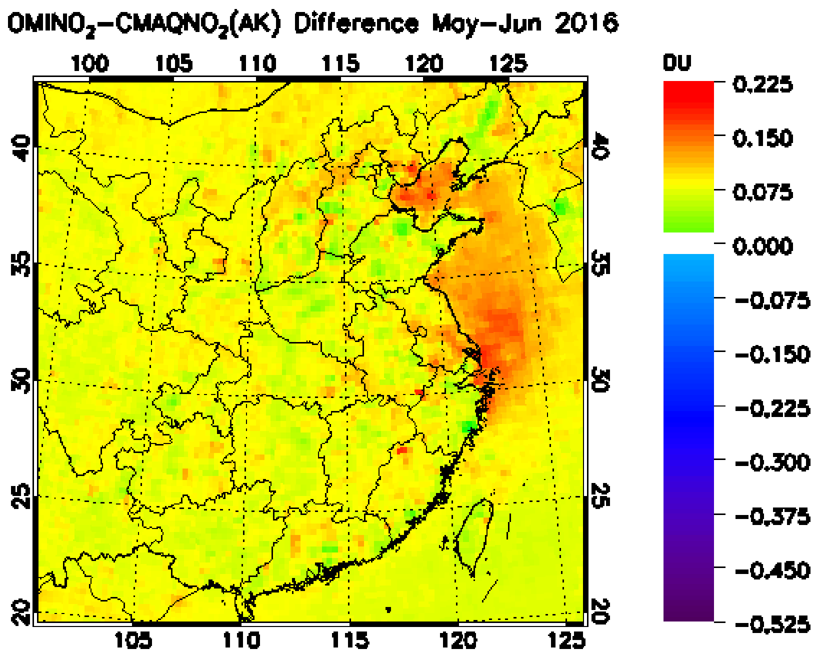

b)

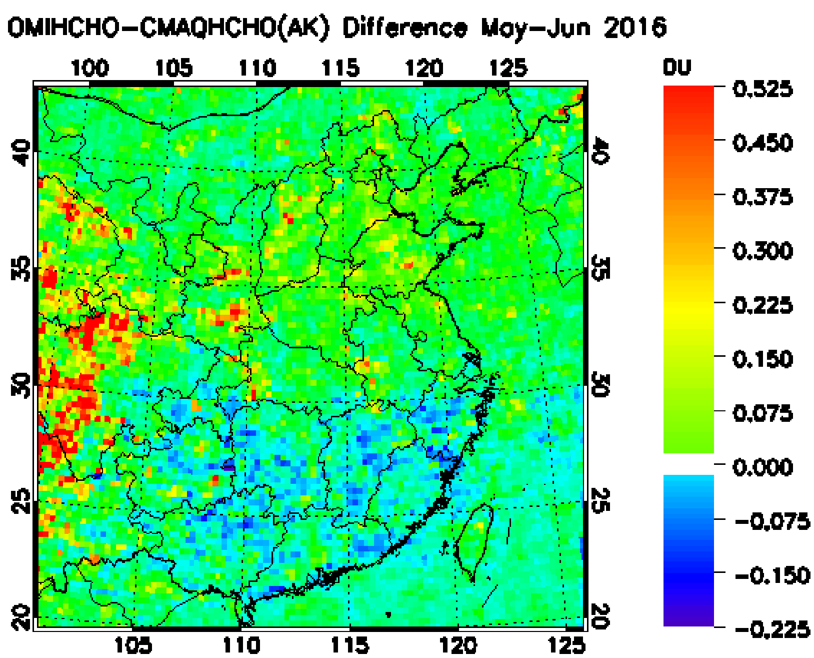

c)

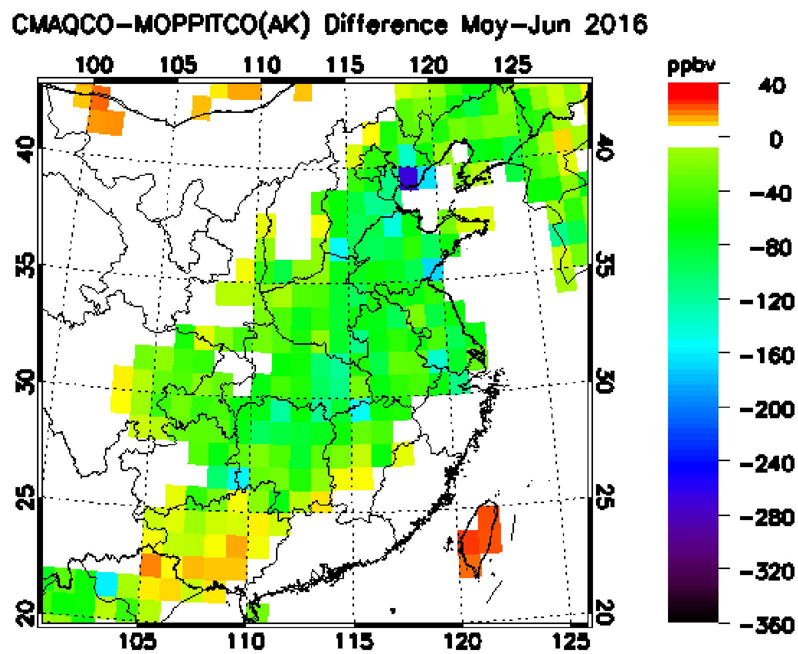

Figure S8. Similar as Figure 10, but shows differences between CMAQ_baseline and CMAQ_all runs with respect to surface observations. a) O_3, b) CO, c) NO2, d) NOx, e) HCHO

a)

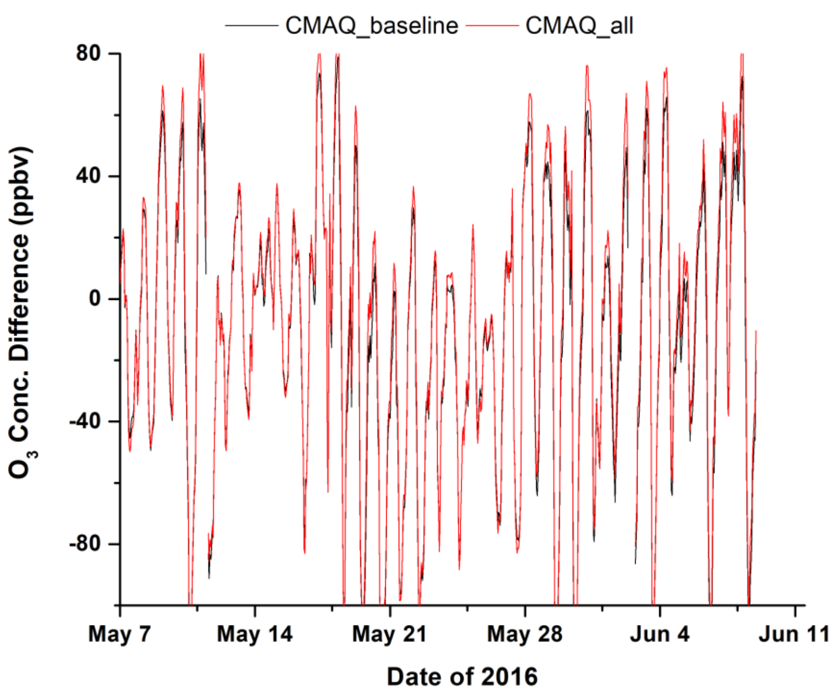

b)

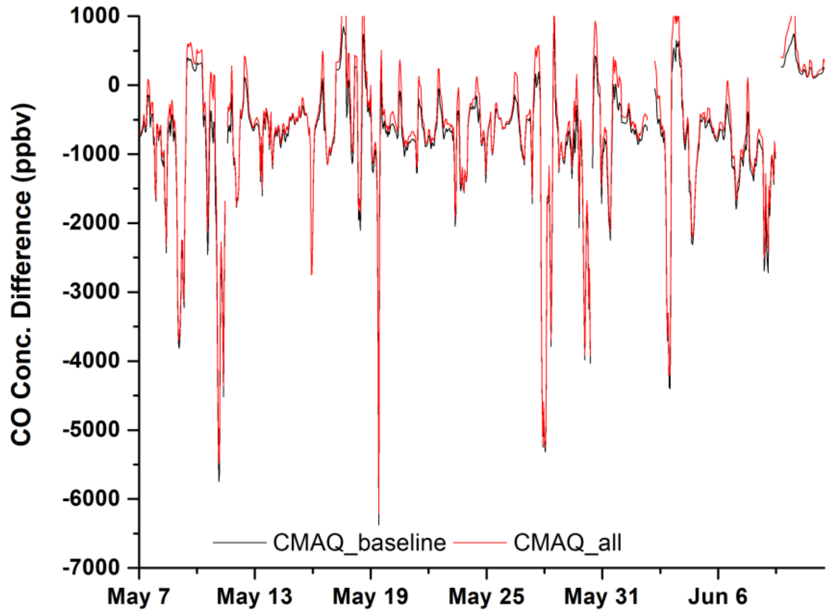

CO Conc. Difference (ppbv)
1000
0
-1000
-2000
-3000
-4000
-5000
-6000
-7000
CMAQ_baseline
CMAQ_all
May 7
May 13
May 19
May 25
May 31
Jun 6

c)

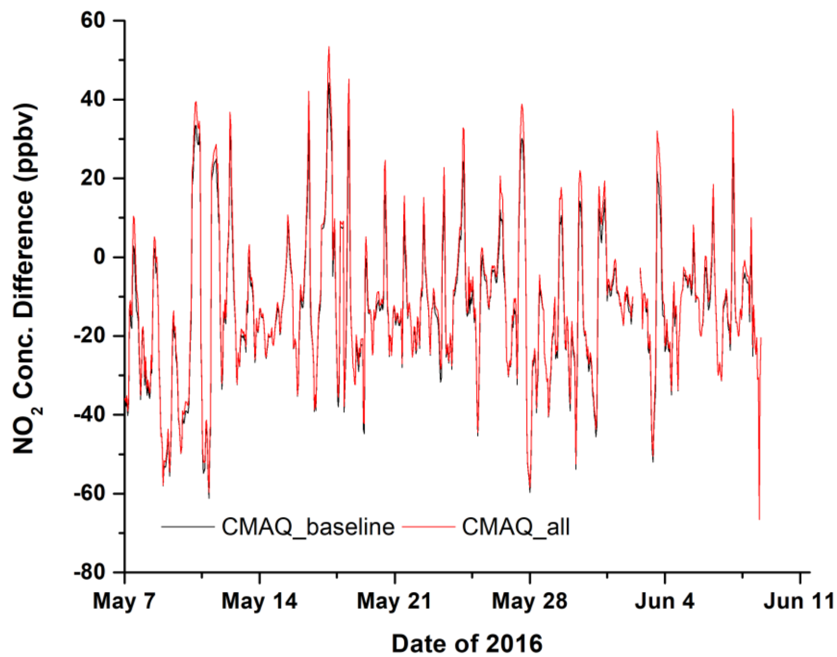

NO2 Conc. Difference (ppbv)
60
40
20
0
-20
-40
-60
-80
CMAQ_baseline
CMAQ_all
May 7
May 14
May 21
May 28
Jun 4
Jun 11
Date of 2016

d)

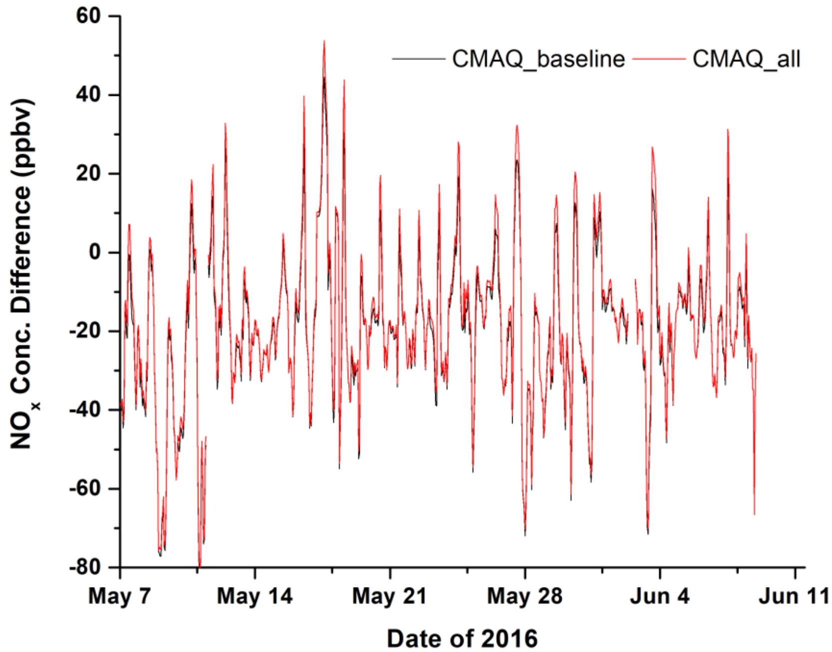
CMAQ_baseline
CMAQ_all
NO_x Conc. Difference (ppbv)
60
40
20
0
-20
-40
-60
-80
May 7
May 14
May 21
May 28
Jun 4
Jun 11
Date of 2016

e)

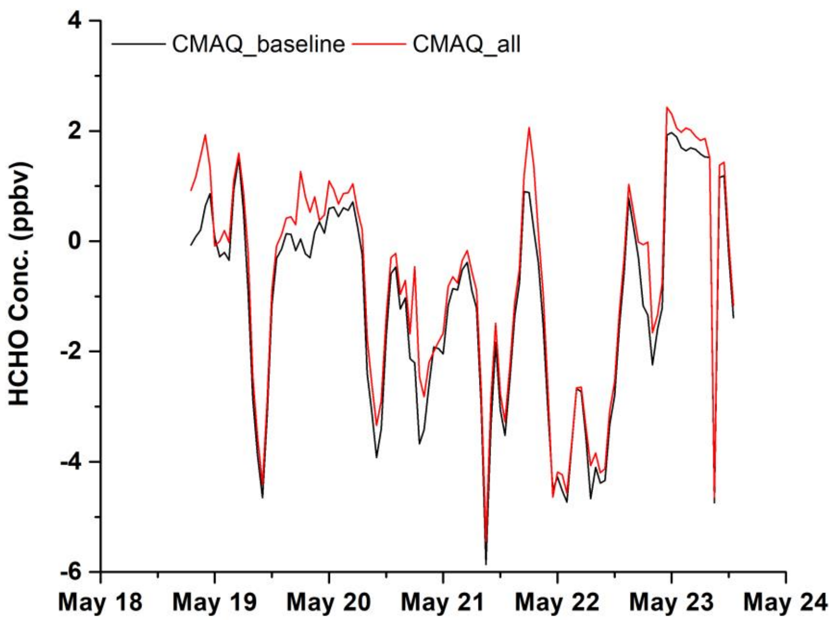
CMAQ_baseline
CMAQ_all
HCHO Conc. (ppbv)
4
2
0
-2
-4
-6
May 18
May 19
May 20
May 21
May 22
May 23
May 24

Figure S9. Similar as Figure S3, but shows concentrations of air pollutants from all 6 CMAQ simulations.

a)

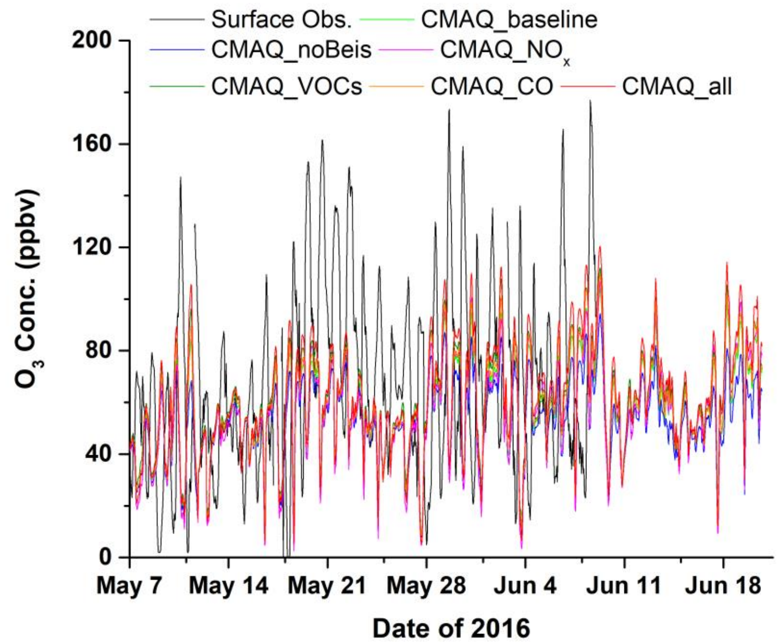

b)

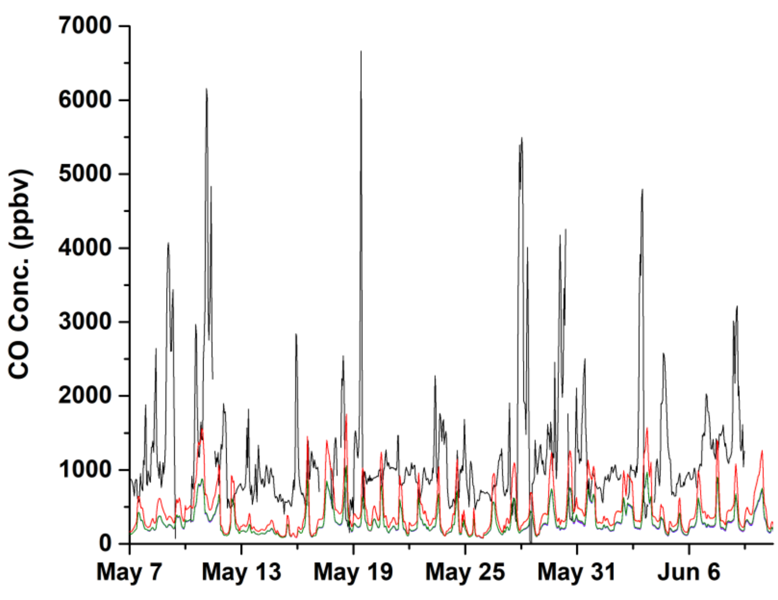

c)

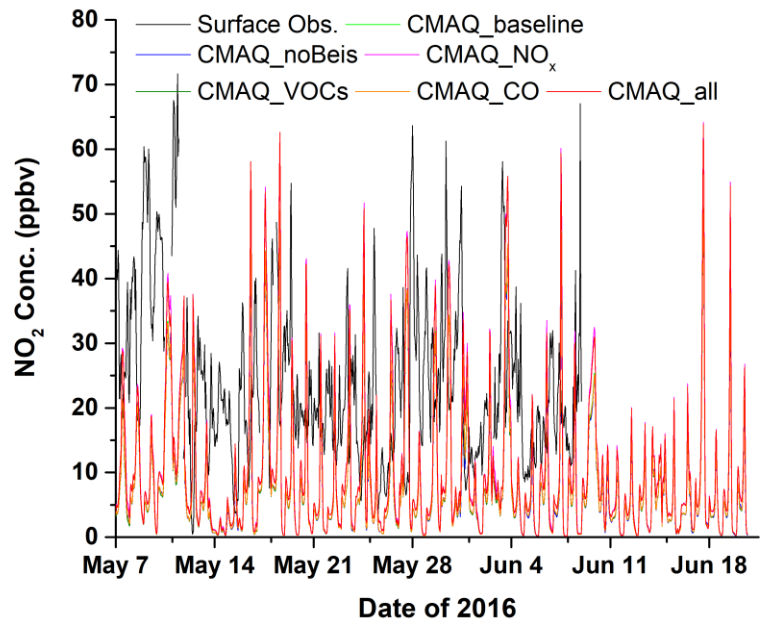
Surface Obs.
CMAQ_baseline
CMAQ_noBeis
CMAQ_NO$_x$
CMAQ_VOCs
CMAQ_CO
CMAQ_all
NO_2 Conc. (ppbv)
0
10
20
30
40
50
60
70
80
May 7
May 14
May 21
May 28
Jun 4
Jun 11
Jun 18
Date of 2016

d)

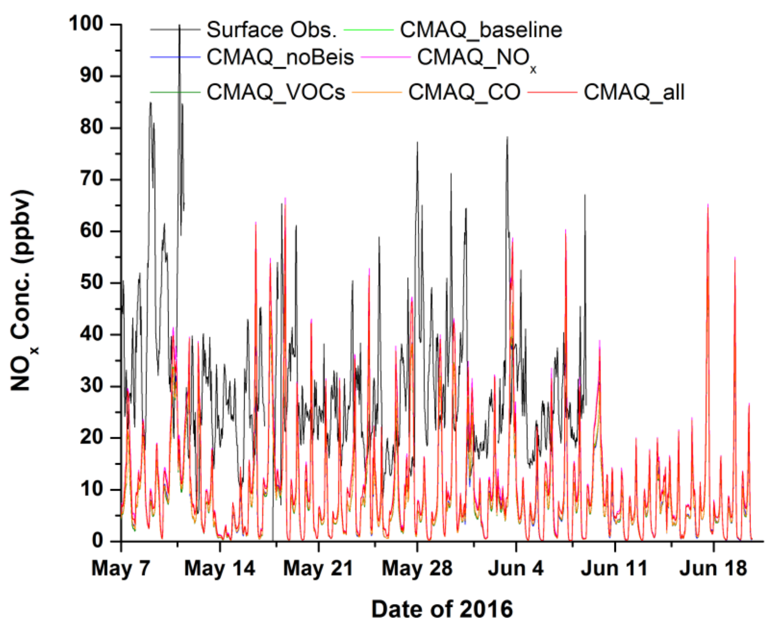
Surface Obs.
CMAQ_baseline
CMAQ_noBeis
CMAQ_NO$_x$
CMAQ_VOCs
CMAQ_CO
CMAQ_all
NO_x Conc. (ppbv)
0
10
20
30
40
50
60
70
80
90
100
May 7
May 14
May 21
May 28
Jun 4
Jun 11
Jun 18
Date of 2016

e)

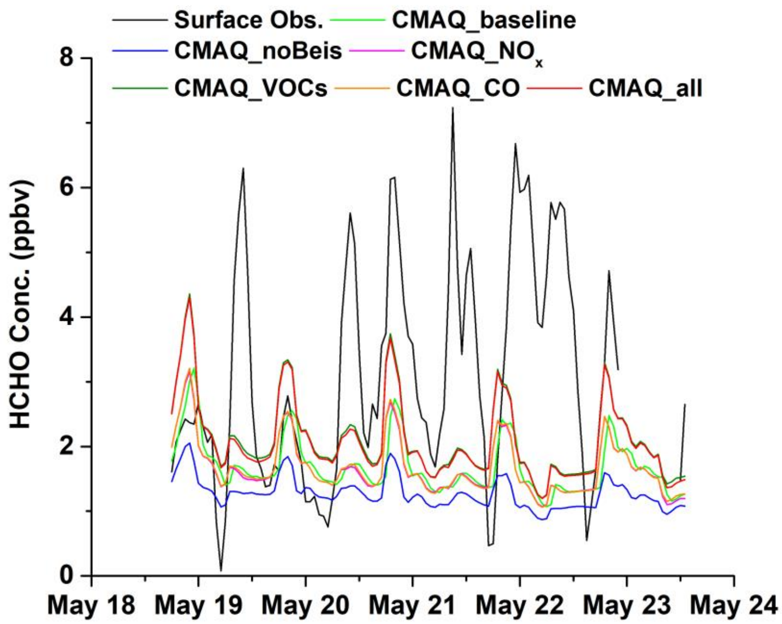

Figure S10. Similar as Figure 4, but shows results from other CMAQ sensitivity experiments.

a) CMAQ_noBEIS

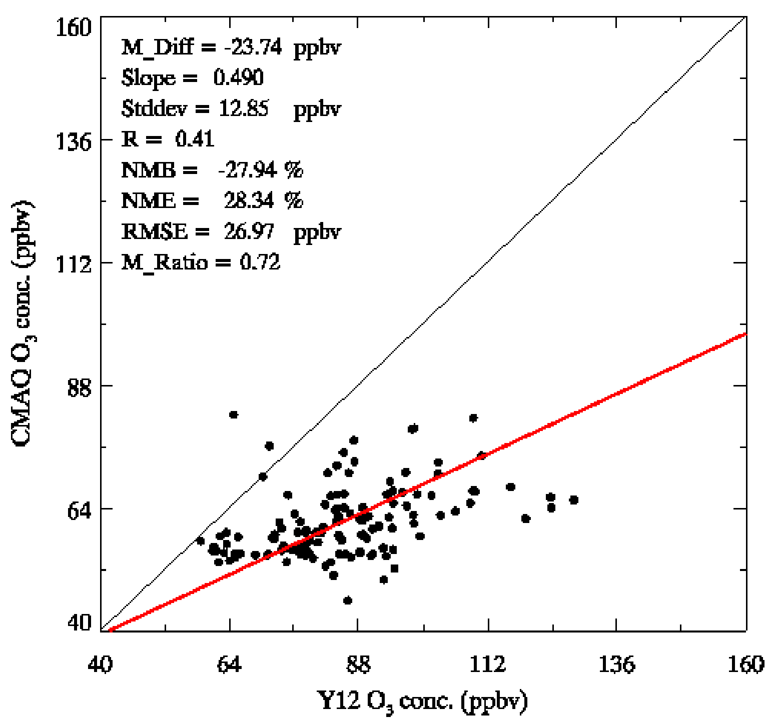

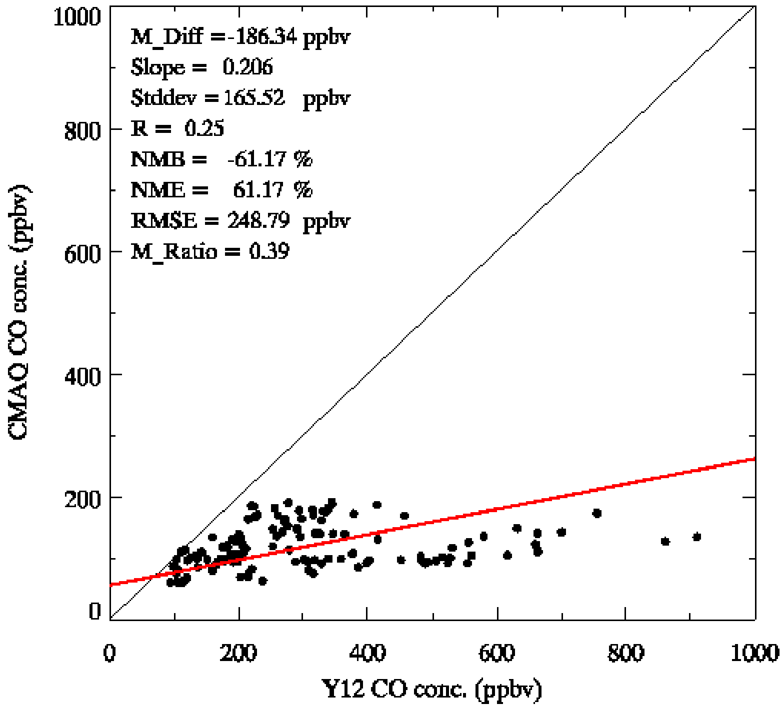
M_Diff =-186.34 ppbv
Slope = 0.206
Stddev = 165.52 ppbv
R = 0.25
NMB = -61.17 %
NME = 61.17 %
RMSE = 248.79 ppbv
M_Ratio = 0.39
CMAQ CO conc. (ppbv)
Y12 CO conc. (ppbv)
0
200
400
600
800
1000

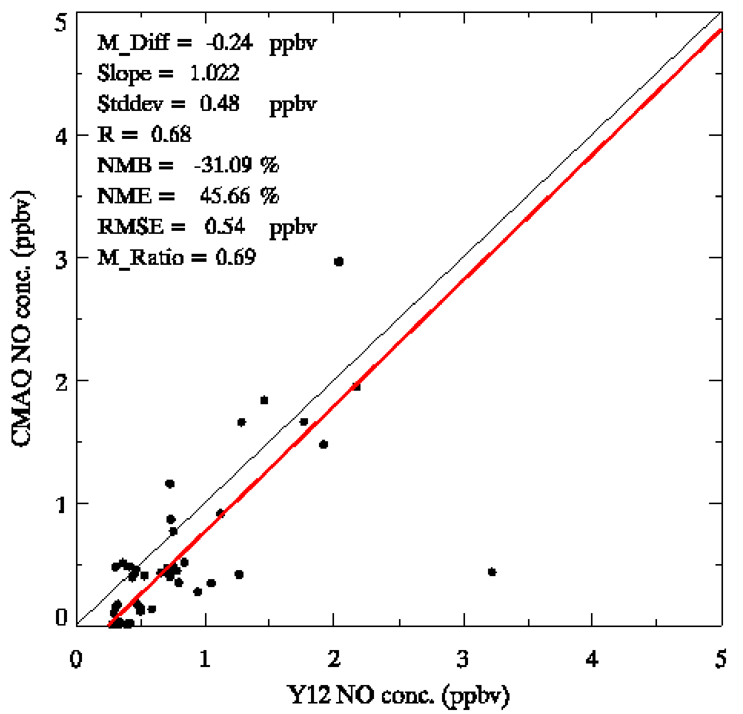
M_Diff = -0.24 ppbv
Slope = 1.022
Stddev = 0.48 ppbv
R = 0.68
NMB = -31.09 %
NME = 45.66 %
RMSE = 0.54 ppbv
M_Ratio = 0.69
CMAQ NO conc. (ppbv)
Y12 NO conc. (ppbv)
0
1
2
3
4
5

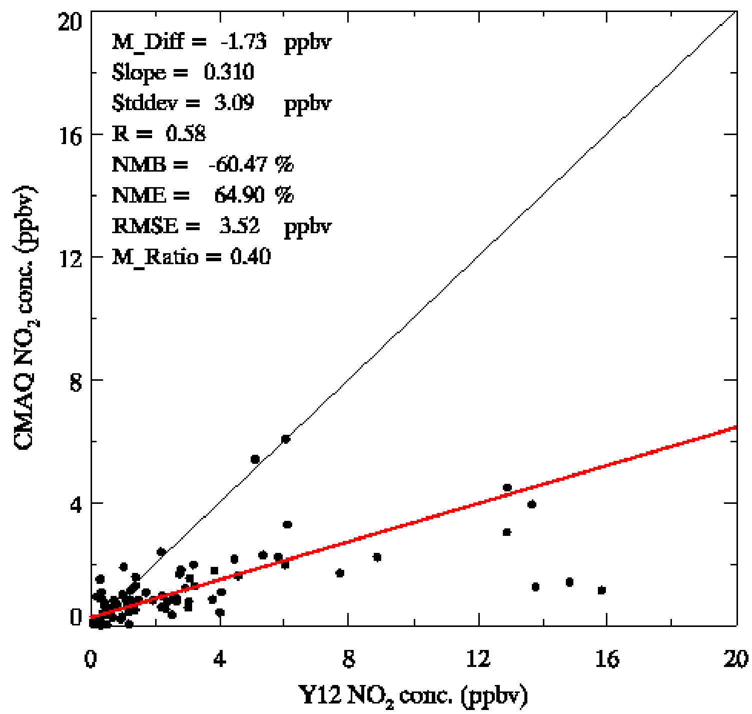
M_Diff = -1.73 ppbv
Slope = 0.310
Stddev = 3.09 ppbv
R = 0.58
NMB = -60.47 %
NME = 64.90 %
RMSE = 3.52 ppbv
M_Ratio = 0.40
CMAQ NO_2 conc. (ppbv)
Y12 NO_2 conc. (ppbv)
0
4
8
12
16
20

b) CMAQ_NOx

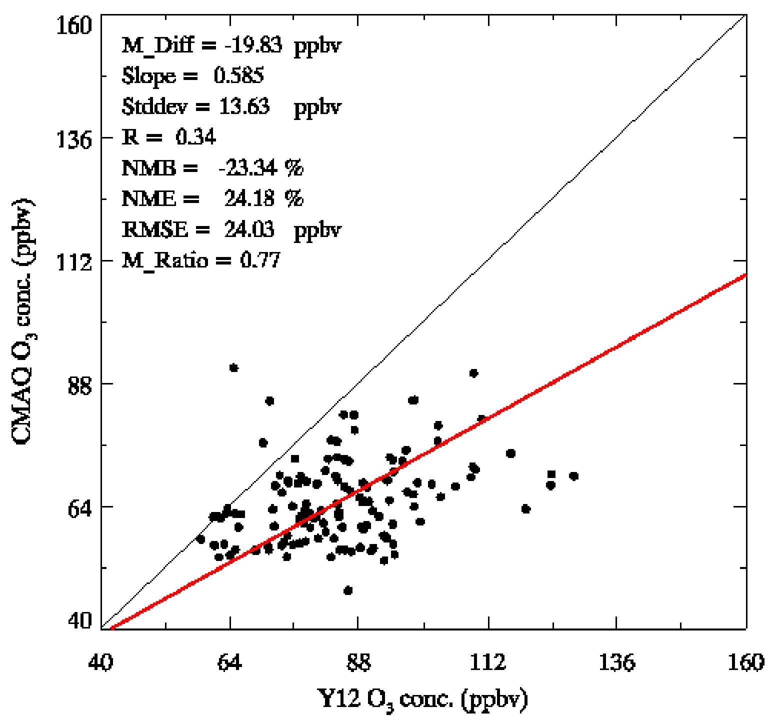
M_Diff = -19.83 ppbv
Slope = 0.585
Stddev = 13.63 ppbv
R = 0.34
NMB = -23.34 %
NME = 24.18 %
RMSE = 24.03 ppbv
M_Ratio = 0.77
CMAQ O_3 conc. (ppbv)
Y12 O_3 conc. (ppbv)
40
64
88
112
136
160

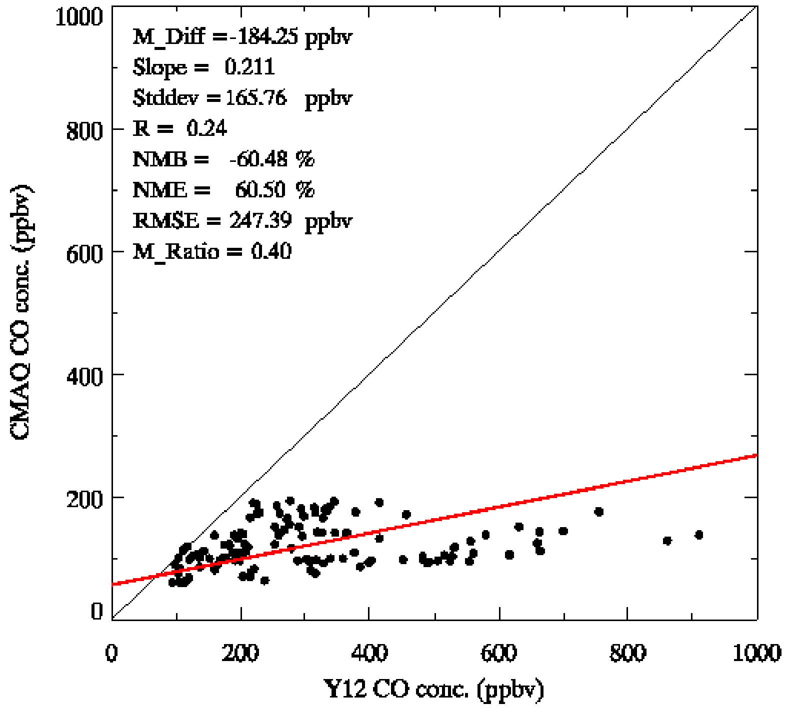
M_Diff =-184.25 ppbv
Slope = 0.211
Stddev = 165.76 ppbv
R = 0.24
NMB = -60.48 %
NME = 60.50 %
RMSE = 247.39 ppbv
M_Ratio = 0.40
CMAQ CO conc. (ppbv)
Y12 CO conc. (ppbv)
0
200
400
600
800
1000

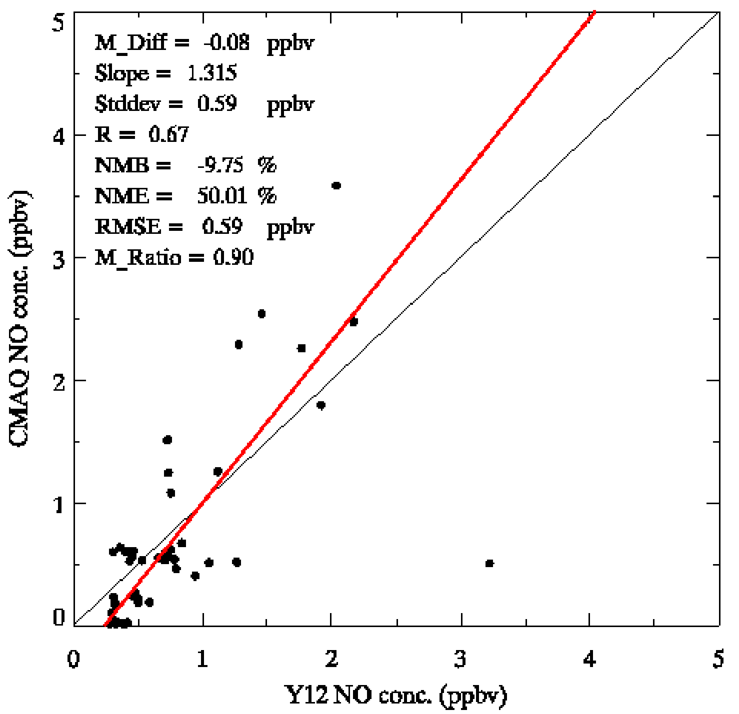
M_Diff = -0.08 ppbv
Slope = 1.315
Stddev = 0.59 ppbv
R = 0.67
NMB = -9.75 %
NME = 50.01 %
RMSE = 0.59 ppbv
M_Ratio = 0.90
CMAQ NO conc. (ppbv)
Y12 NO conc. (ppbv)
0
1
2
3
4
5

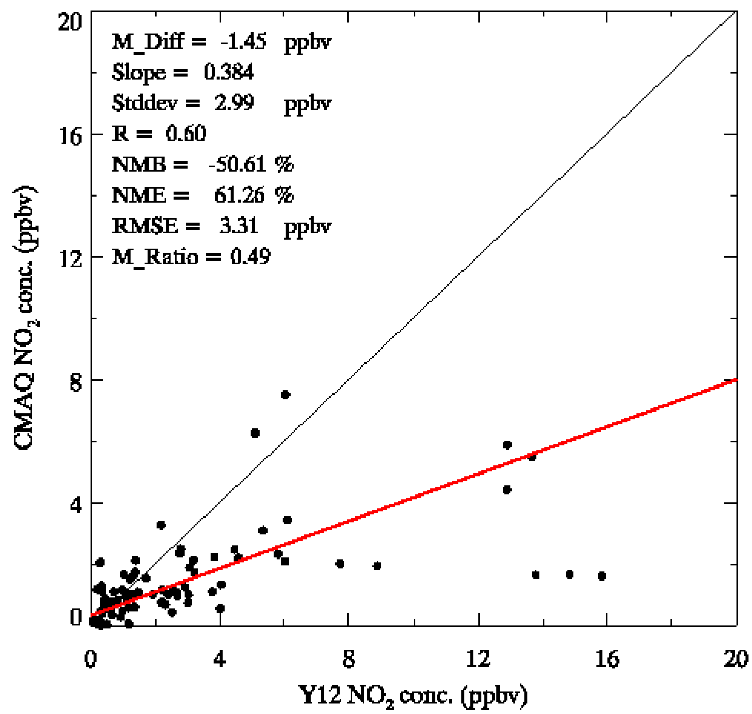
M_Diff = -1.45 ppbv
Slope = 0.384
Stddev = 2.99 ppbv
R = 0.60
NMB = -50.61 %
NME = 61.26 %
RMSE = 3.31 ppbv
M_Ratio = 0.49
CMAQ NO_2 conc. (ppbv)
Y12 NO_2 conc. (ppbv)
0
4
8
12
16
20

c) CMAQ_VOCs

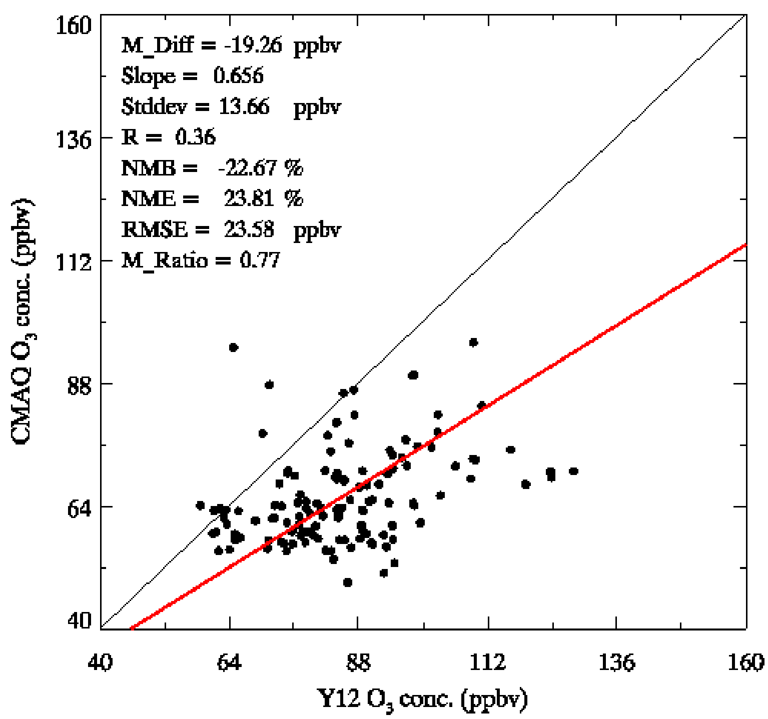
M_Diff = -19.26 ppbv
Slope = 0.656
Stddev = 13.66 ppbv
R = 0.36
NMB = -22.67 %
NME = 23.81 %
RMSE = 23.58 ppbv
M_Ratio = 0.77
CMAQ O_3 conc. (ppbv)
Y12 O_3 conc. (ppbv)
40
64
88
112
136
160

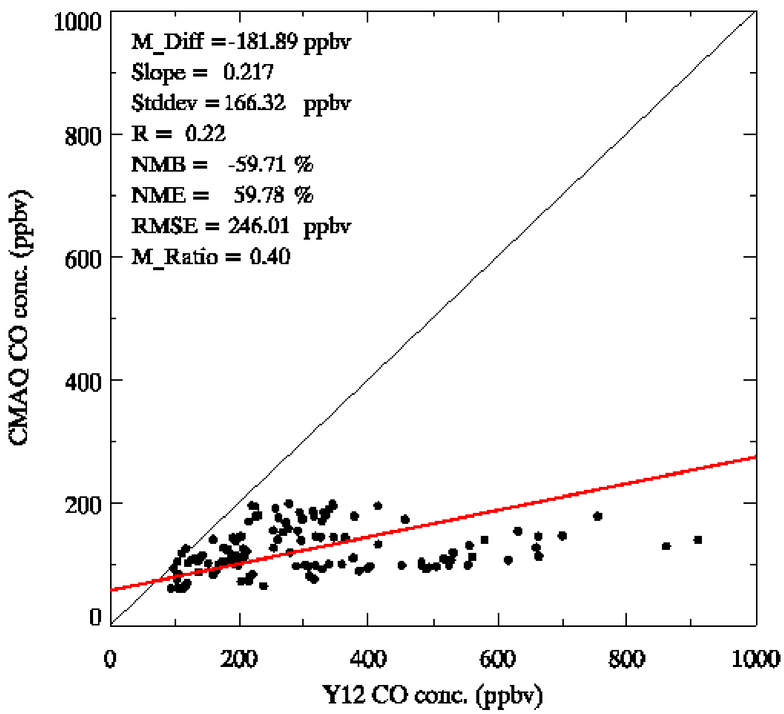
M_Diff =-181.89 ppbv
Slope = 0.217
Stddev = 166.32 ppbv
R = 0.22
NMB = -59.71 %
NME = 59.78 %
RMSE = 246.01 ppbv
M_Ratio = 0.40
CMAQ CO conc. (ppbv)
Y12 CO conc. (ppbv)
0
200
400
600
800
1000

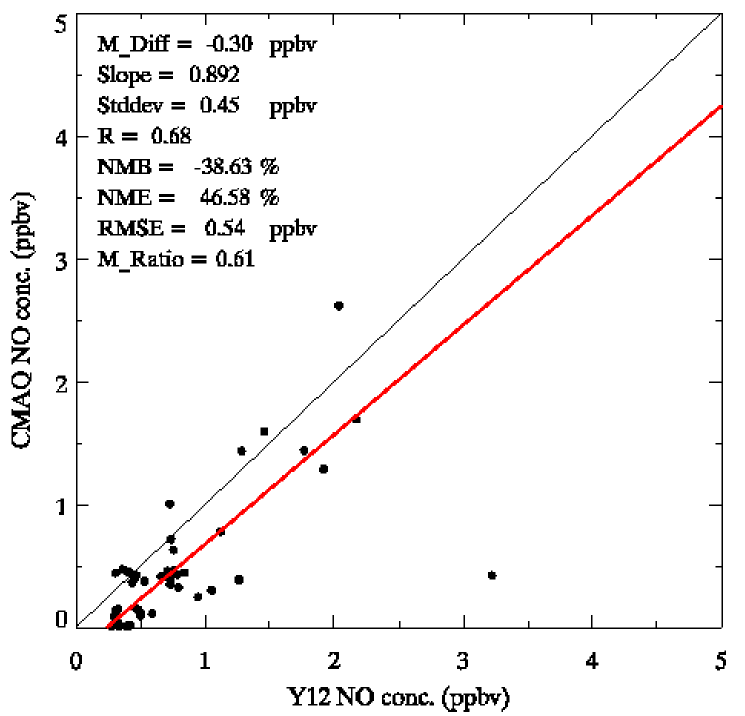
M_Diff = -0.30 ppbv
Slope = 0.892
Stddev = 0.45 ppbv
R = 0.68
NMB = -38.63 %
NME = 46.58 %
RMSE = 0.54 ppbv
M_Ratio = 0.61
CMAQ NO conc. (ppbv)
Y12 NO conc. (ppbv)
0
1
2
3
4
5

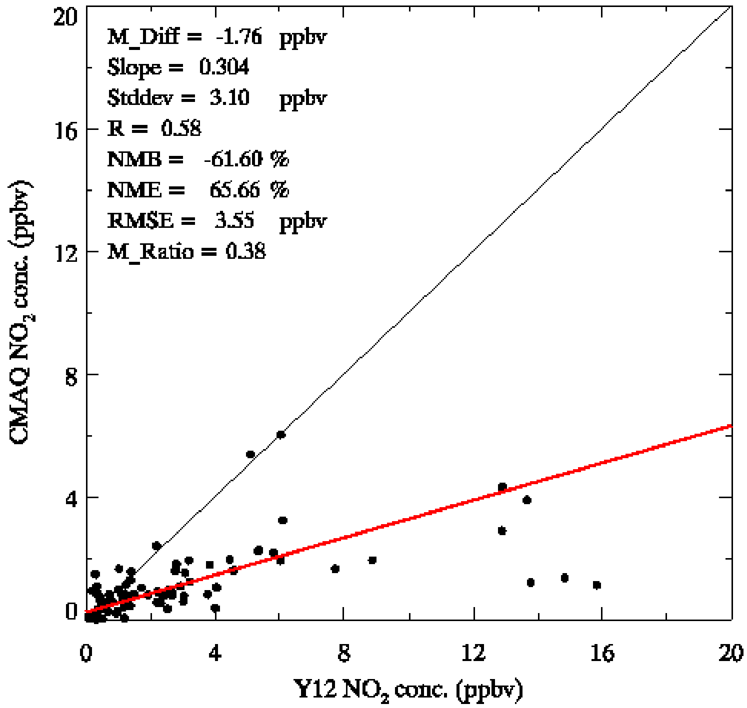
M_Diff = -1.76 ppbv
Slope = 0.304
Stddev = 3.10 ppbv
R = 0.58
NMB = -61.60 %
NME = 65.66 %
RMSE = 3.55 ppbv
M_Ratio = 0.38
CMAQ NO_2 conc. (ppbv)
Y12 NO_2 conc. (ppbv)
0
4
8
12
16
20

d) CMAQ_CO

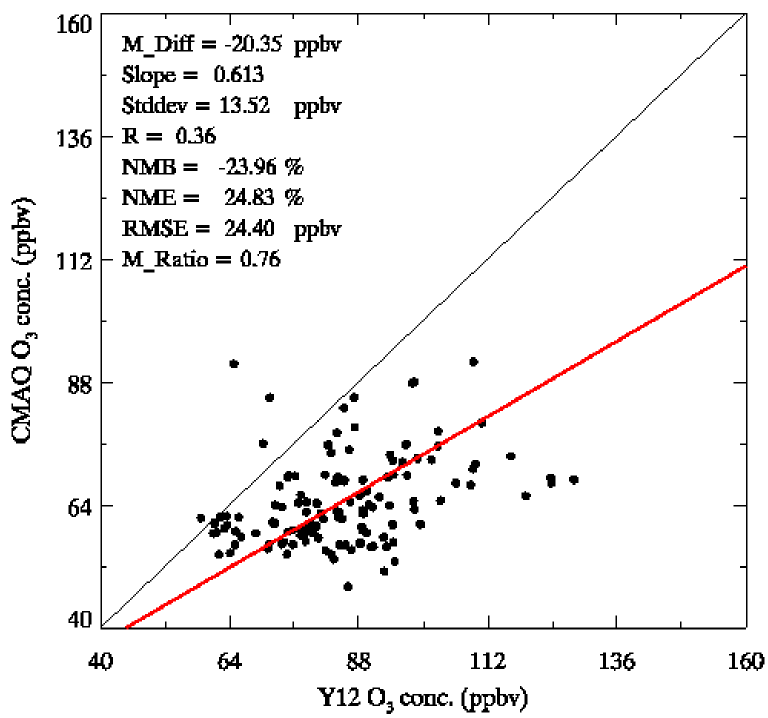
M_Diff = -20.35 ppbv
Slope = 0.613
Stddev = 13.52 ppbv
R = 0.36
NMB = -23.96 %
NME = 24.83 %
RMSE = 24.40 ppbv
M_Ratio = 0.76
CMAQ O_3 conc. (ppbv)
Y12 O_3 conc. (ppbv)
40
64
88
112
136
160

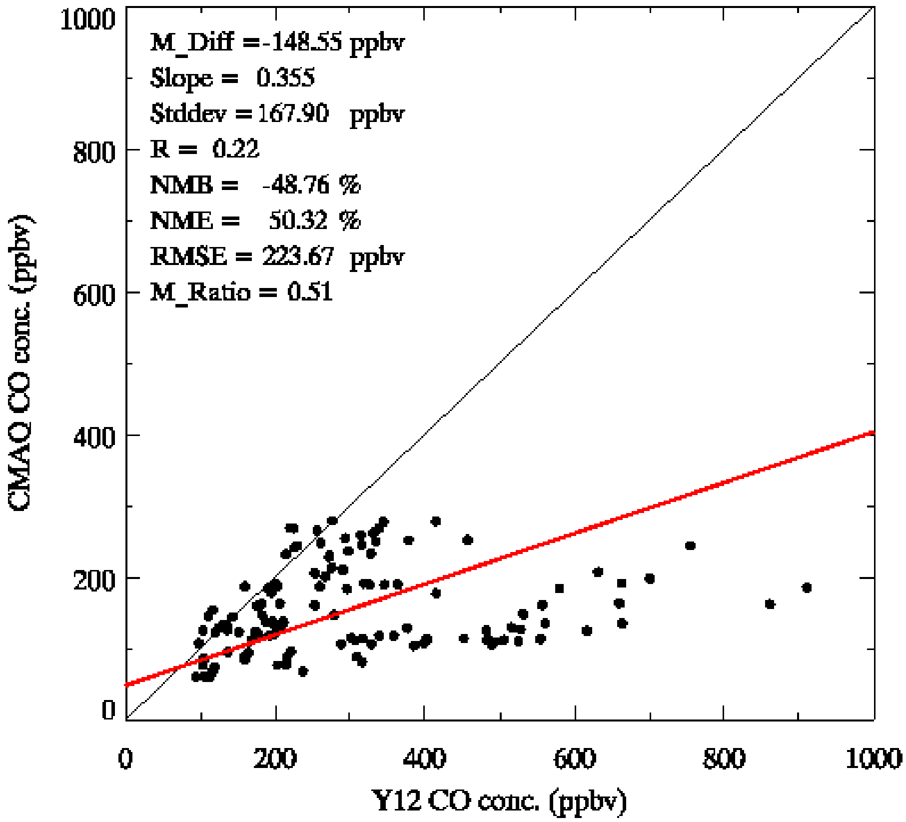
M_Diff =-148.55 ppbv
Slope = 0.355
Stddev = 167.90 ppbv
R = 0.22
NMB = -48.76 %
NME = 50.32 %
RMSE = 223.67 ppbv
M_Ratio = 0.51
CMAQ CO conc. (ppbv)
Y12 CO conc. (ppbv)
0
200
400
600
800
1000

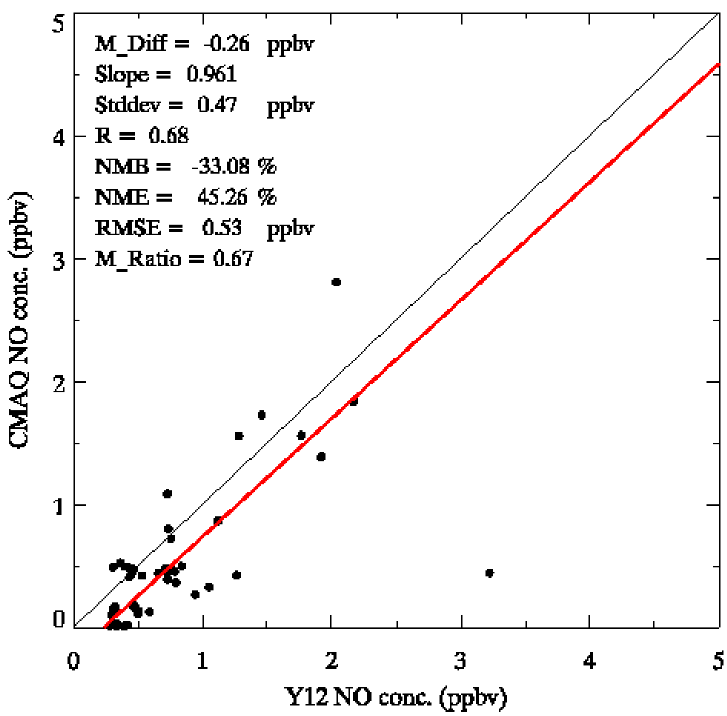
M_Diff = -0.26 ppbv
Slope = 0.961
Stddev = 0.47 ppbv
R = 0.68
NMB = -33.08 %
NME = 45.26 %
RMSE = 0.53 ppbv
M_Ratio = 0.67
CMAQ NO conc. (ppbv)
Y12 NO conc. (ppbv)
0
1
2
3
4
5

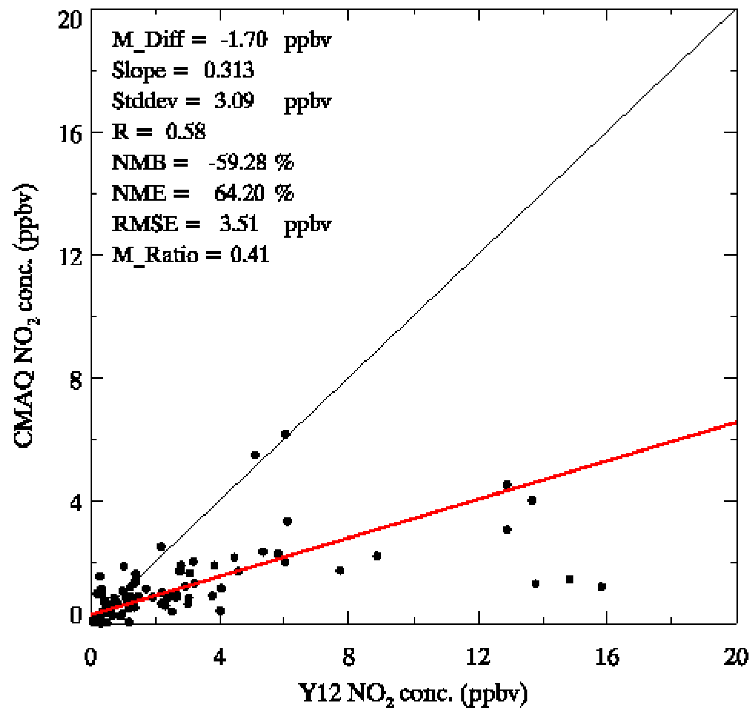
M_Diff = -1.70 ppbv
Slope = 0.313
Stddev = 3.09 ppbv
R = 0.58
NMB = -59.28 %
NME = 64.20 %
RMSE = 3.51 ppbv
M_Ratio = 0.41
CMAQ NO_2 conc. (ppbv)
Y12 NO_2 conc. (ppbv)
0
4
8
12
16
20

e) CMAQ_all

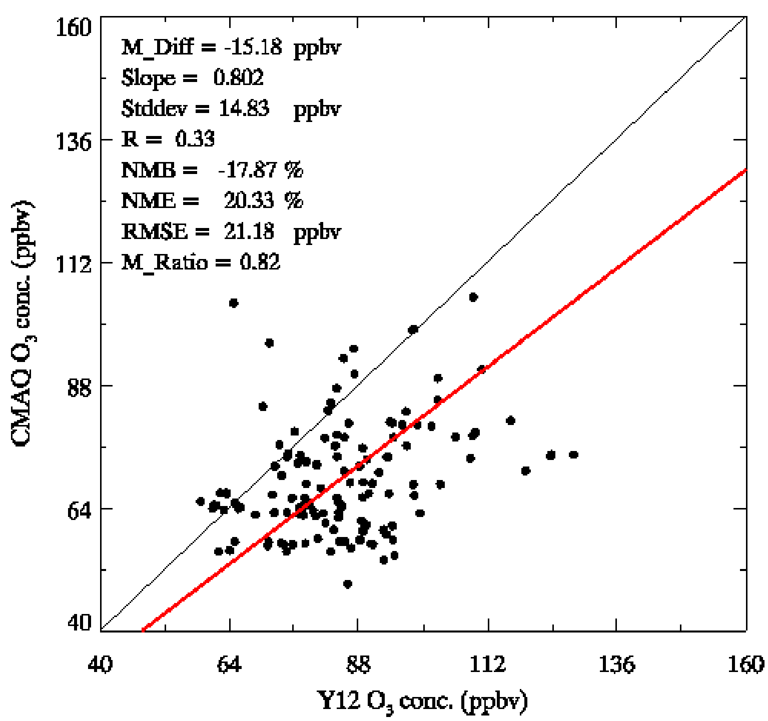
M_Diff = -15.18 ppbv
Slope = 0.802
Stddev = 14.83 ppbv
R = 0.33
NMB = -17.87 %
NME = 20.33 %
RMSE = 21.18 ppbv
M_Ratio = 0.82
CMAQ O_3 conc. (ppbv)
Y12 O_3 conc. (ppbv)
40
64
88
112
136
160

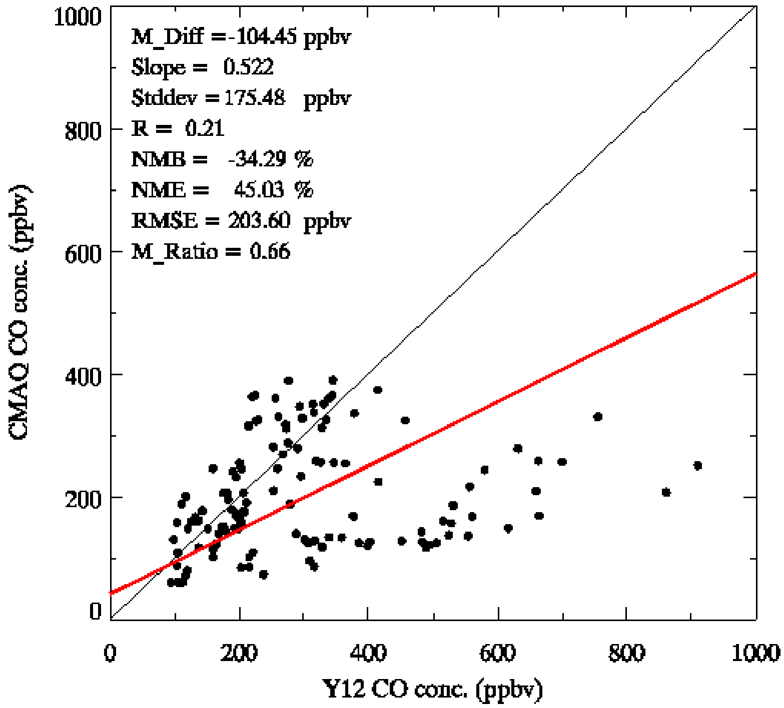
M_Diff =-104.45 ppbv
Slope = 0.522
Stddev = 175.48 ppbv
R = 0.21
NMB = -34.29 %
NME = 45.03 %
RMSE = 203.60 ppbv
M_Ratio = 0.66
CMAQ CO conc. (ppbv)
Y12 CO conc. (ppbv)
0
200
400
600
800
1000

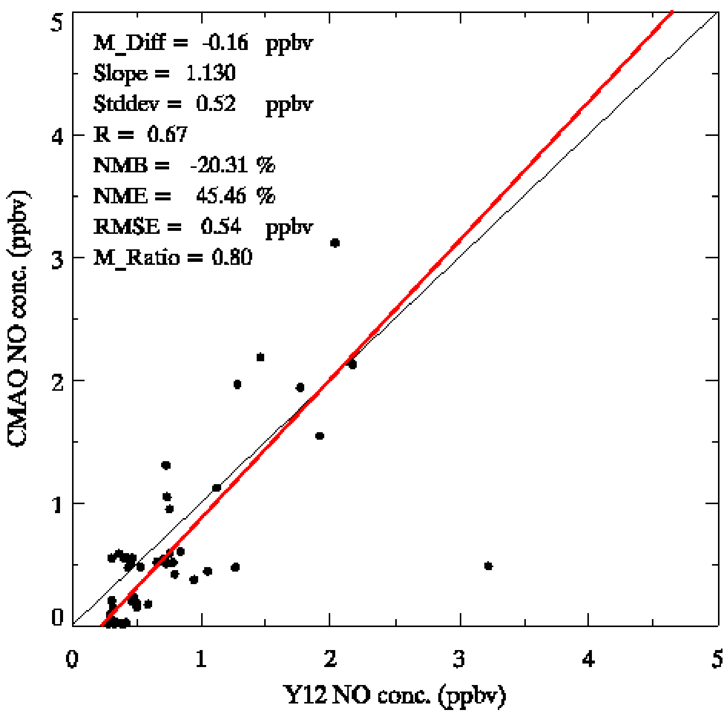
M_Diff = -0.16 ppbv
Slope = 1.130
Stddev = 0.52 ppbv
R = 0.67
NMB = -20.31 %
NME = 45.46 %
RMSE = 0.54 ppbv
M_Ratio = 0.80
CMAQ NO conc. (ppbv)
Y12 NO conc. (ppbv)
0
1
2
3
4
5

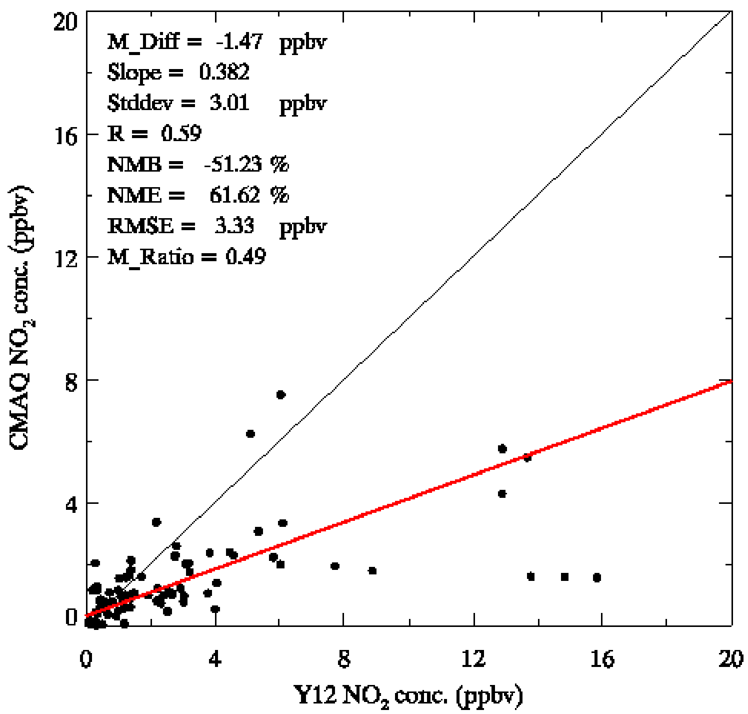
M_Diff = -1.47 ppbv
Slope = 0.382
Stddev = 3.01 ppbv
R = 0.59
NMB = -51.23 %
NME = 61.62 %
RMSE = 3.33 ppbv
M_Ratio = 0.49
CMAQ NO_2 conc. (ppbv)
Y12 NO_2 conc. (ppbv)
0
4
8
12
16
20

148